A Compact Optical Sensor for Explosive Detection Based on NIR Luminescent Quantum Dots

F. Mitri[1], A. De Iacovo[1*], S. De Santis[1], C. Giansante[2], D. Spirito[3], G. Sotgiu[1], and L. Colace[1]

[1)] Department of Engineering, University Roma Tre, Via Vito Volterra 62, 00146, Rome, Italy
[2)] CNR Nanotec, Istituto di Nanotecnologia, Via Monteroni, Lecce 73100, Italy.
[3)] IHP - Leibniz Institut für innovative Mikroelektronik, Im Technologiepark 25, 15236 Frankfurt (Oder), Germany.
(*Electronic mail: andrea.deiacovo@uniroma3.it)

Detection of explosive traces in the vapor phase is of primary importance for safety and security in several environments. Different detection methods with high sensitivity are available on the market, but they are typically expensive and require specialized personnel to be operated. Here we propose a compact, low-cost sensor for explosive detection based on the photoluminescence (PL) quenching of solid-state PbS quantum dot solids casted from the solution phase on a silicon substrate. We demonstrate the sensor capability to detect nitrobenzene vapor at concentration as low as 445 ppb in air at room temperature, overcoming the performance of other state-of-the-art quantum dot-based PL sensors for nitroaromatic compounds. Moreover, the proposed system can be realized with off-the-shelf electronics and does not need any additional laboratory equipment to be operated, thus paving the way for its deployment in distributed sensor networks.

Nitroaromatic compounds (NACs) are a global concern for their use as explosives and for their high toxicity [1]. Traditional analytical NACs detection methods include optical and electrochemical analysis as well as spectroscopy-based techniques[2–4]. Despite the high sensitivity of these methods, they require time consuming sample preparation and measurement procedures in addition to expensive instruments and trained technical staff. For these reasons, analytical techniques are typically confined in lab environments and in highly sensitive spots such as airports. Recently, a different detection approach based on fluorescent materials attracted much attention and demonstrated great potential[5,6]. When interactions with explosives occur, photoluminescence (PL) can change in terms of intensity (quenching or enhancement), wavelength, anisotropy, or lifetime, depending on the NACs concentration[7]. Among the different classes of materials, Quantum Dots (QDs) have also been investigated over the past few years[8]. Thanks to their strong quantum confinement, QDs exhibit unique optical properties such as high absorption and emission along with quantum-size tunability[9]. They can be easily fabricated and functionalized[10] and, thanks to the high surface-to-volume ratio, they show outstanding reactivity with several chemical species[11]. Most of the QD-based sensors for trace explosive detection are limited to water or soil samples and require direct contact with the compounds, whereas vapor detection remains a challenge upon which only few examples are reported in literature[12–14] due to the very low vapor pressure of NACs at room temperature. Moreover, QD-based NACs sensors reported in literature and exploiting the PL quenching still rely on external instrumentation to quantify the change in PL intensity, hence determining the NACs' concentration[15,16]. Here we present a NACs detection system where the evaluation of the PL quenching is obtained with a photodetector directly integrated with the QD-based PL probe. The proposed device exploits the PL quenching of amine-capped PbS QDs deposited on a silicon substrate for vapor detection of nitrobenzene (NB), selected in this work as a widely employed representative NAC. The system is assembled with low-cost and low-power components, including a blue light emitting diode (LED) and a germanium photodetector (Ge PD) to make it suitable for a large-scale deployment. Compared to previously reported devices based on QD PL quenching, the proposed system can be easily operated in a standalone mode, without the need of specific instrumentation or interaction with a human operator. Moreover, the device is reusable and portable since the NAC detection process is reversible and the device can be battery powered.

The proposed sensor-system is shown in Fig. 1, and it is assembled from different components:

1. 3D-printed measuring chamber, with air in-let and out-let connectors and an internal volume of 10 mL
2. PL-QD-coated silicon substrate with dimensions 9 x 9 x 0.7 mm
3. Blue LED, providing optical pump for QD PL, positioned at a distance of 20 mm on top of the Si substrate
4. Ge photodiode, fixed to the chamber and completely covered by the Si substrate.

Fig. 1a shows the device's operating scheme. Blue light (emission peak at λ=465 nm) emitted from the LED impinges onto the QD. The QD have been specifically synthesized with a diameter of about 4.7 nm in order to produce a near infrared (NIR) PL peak centered at 1400 nm; synthesis details are reported elsewhere[17]. The silicon substrate is opaque for the blue light, but it is transparent for the NIR radiation emitted by the QD. Therefore, the emitted photons can reach the Ge photodetector which, in turn, generates a photocurrent proportional to the PL intensity. The silicon chip acts both as a deposition substrate for the QDs and as an optical filter, hindering the blue light from reaching the Ge photodiode, thus ensuring no crosstalk between the pump signal and the PL signal. Fig. 1b and 1c show the schematic cross-section of the system assembly and a photography.

PL devices were fabricated with a layer-by-layer approach by spin-coating the QD suspension alternated with a solid-state ligand exchange procedure with ethylenediamine (EDA). EDA was chosen as a sensitizing agent for its good affinity with the surface of the QDs and for its amenability to form Meisenheimer-like compounds with the electron-poor nitrobenzene rings, such as those typically present in NACs. Moreover, amine-capped nanoparticles have been already employed in the past for the realization of highly selective fluorescent probes and chemiresistors for NACs[18,19]. The thickness of the QD layer is ~200 nm, as measured by optical profilometry.

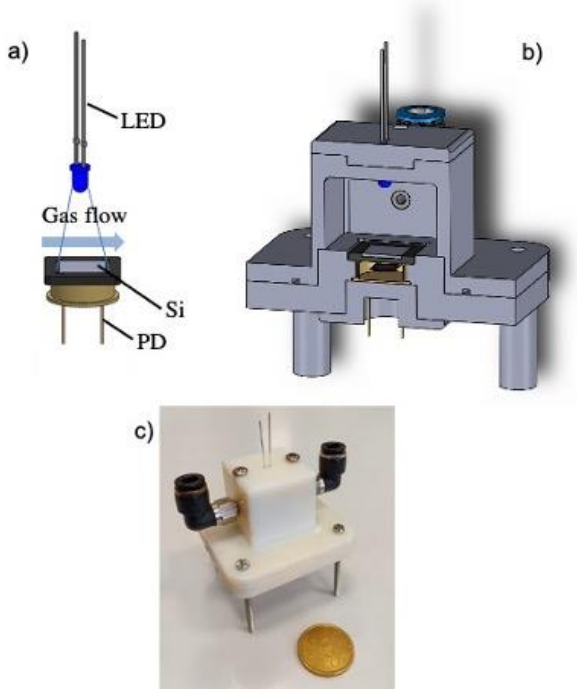

FIG. 1. (a) Schematic of the optical arrangement. (b) 3D model and (c) photography of the measurement chamber.

The QD film was characterized to determine its emission spectrum and verify that the PL peak was at a suitable wavelength. Fig. 2a shows the PL spectrum of the QDs as deposited on the silicon substrate. The spectrum was acquired by exciting at a wavelength of 532 nm, and using a spectrometer optimized for IR measurements (Horiba iHR320), equipped with an extended-InGaAs detector and a 600 lines/mm grating. Fig. 2 also shows the normalized transmittance of the Si substrate (as calculated from the Si thickness and the tabulated complex index of refraction) and the spectral responsivity of the Ge photodiode, together with the emission spectrum of the LED (both provided by the devices datasheets). By design, the pump radiation falls within the low-transmission band of the Si substrate, whereas the PL signal is centered at a high-transmission wavelength and within the responsivity spectrum of the Ge photodiode.

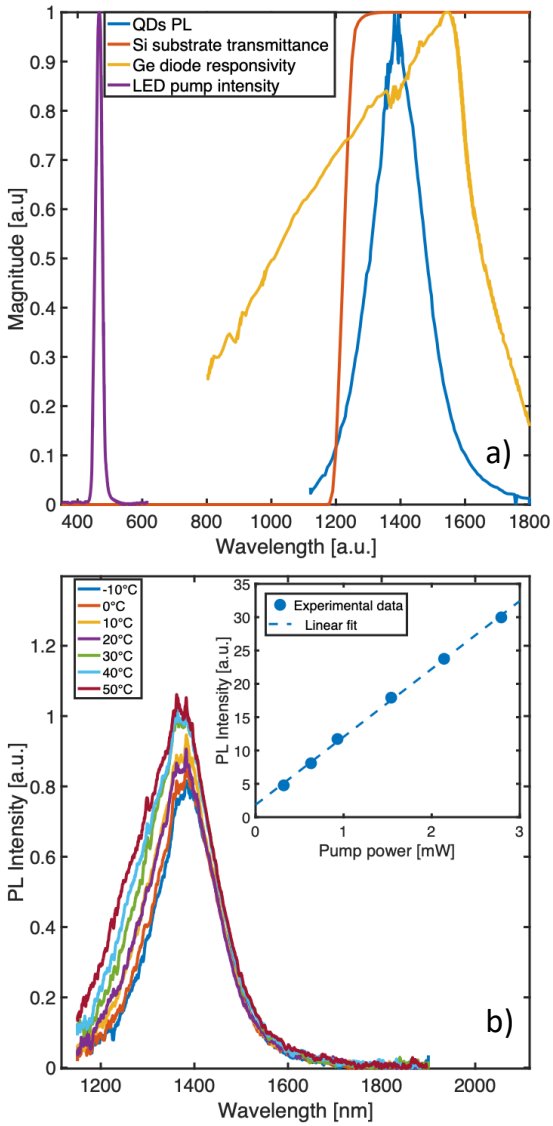

FIG. 2. (a) Comparison of the QD-film PL spectrum, Si substrate's transmission, Ge diode's responsivity and LED pump emission spectrum. All curves are normalized to their maximum. (b) PLspectra at different temperatures and integrated PL intensity vs. pump optical power (inset).

The PL spectrum showed a weak temperature dependence, with a slight blue-shift of the peak intensity at higher temperatures (Fig. 2b). However, the emission spectrum remained centered near 1400 nm, thus confirming device operation in a wide temperature range (-10/+50 °C). Finally, the inset of Fig. 2b shows the variation of the integrated optical power of the PL vs. pump power and the relative linear fit. The observed linear relationship suggests that the device was operated far from any optical absorption saturation regime.
The device response upon exposure to NACs was measured with a custom set-up, schematically shown in Fig. 3. The LED emission intensity was modulated by means of a 520 Hz, 0.5 Vrms sine oscillator and the photocurrent from the Ge photodiode was amplified with a 10 kV/A trans-impedance amplifier. The amplified signal and the LED modulation signal were connected to a demodulation circuit for coherent voltage measurement and data transfer to a personal computer.

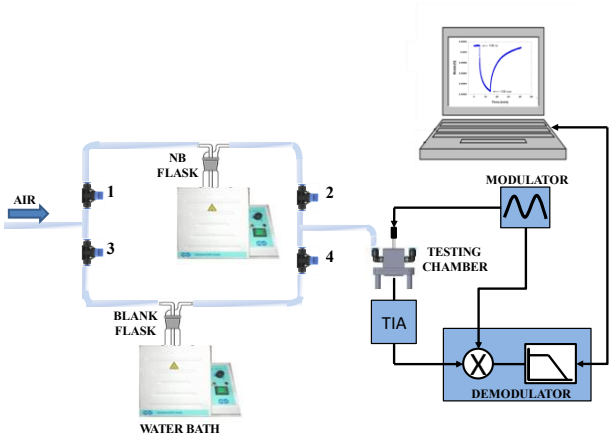

FIG. 3. Schematic representation of the experimental set-up.

The device was characterized at constant temperature (25 °C) and relative humidity (30%), with an 800 mL/min air flow. The LED optical power was 1 mW. Four manual valves were employed to fill the measurement chamber with clean air or with a NB/air mixture. A thermostatic bath (WB-M5 Analogic Thermostatic Bath, Falc Instruments S.r.l) was employed to change the NB concentration. In particular, NB concentrations were calculated from the vapor pressure at different temperatures using the Clausius-Clapeyron equation[20]. In a typical experiment, the measurement chamber was filled with ambient air until the PL signal became stable. Then, the NB gas was allowed to flow through the chamber for the time required to reach a steady state, typically few minutes. Finally, the chamber was purged with clean air to recover the device. Device performance was evaluated through the gas response (S), calculated according to (1),

$$S = \frac{|V|_a - |V|_g}{|V|_a} \times 100 \quad (1)$$

where $|V|_a$ and $|V|_g$ are the amplitude of the measured voltage during clean air flow and NB gas flow, respectively. In addition response time and recovery time of the device were measured, where the former is defined as the time required to reach 90% of the total amplitude change upon NB gas exposure, and the latter is defined as the time required to reach 10% of the total amplitude change upon NB gas release. Fig. 4a shows a typical variation of the photovoltage signal at a NB concentration of 1.9 ppm, that is the maximum concentration obtainable in a closed container at room temperature. When NB reached the sensor, the amplitude of the photovoltage showed a 1 mV variation (corresponding to a sensor response S=10.3%). As expected, the photovoltage decreased during exposure to the NB, thus showing a quenching of the PL efficiency. After NB purge, full recovery of the photovoltage was observed. Response and recovery time were 7.2 and 14 minutes, respectively.

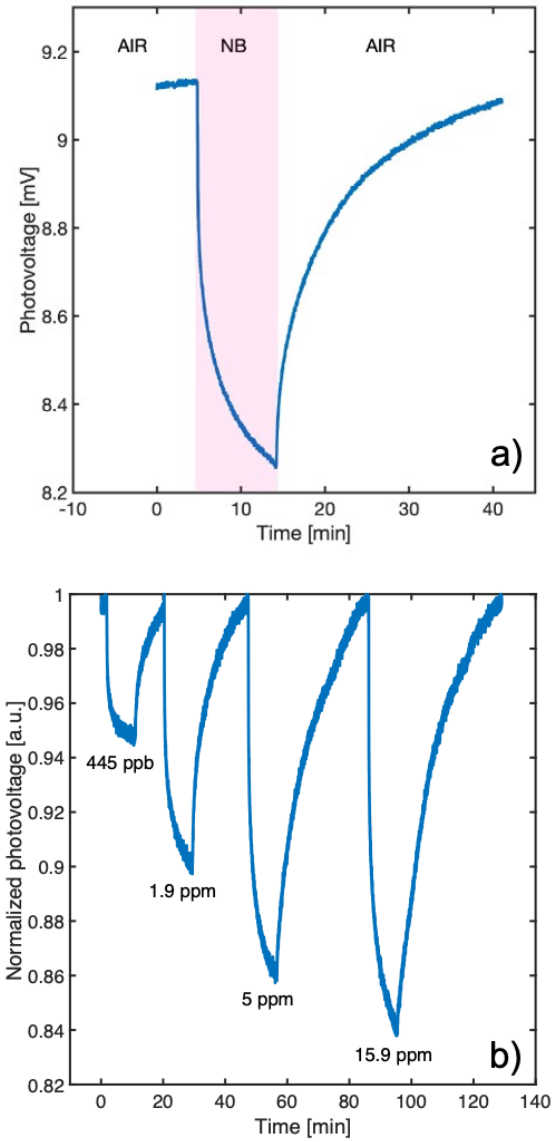

FIG. 4. (a) Amplitude of the photovoltage upon sensor exposure to 1.9 ppm of NB. (b) Amplitude of the photovoltage upon repeated exposure to increasing NB concentrations between 445 ppb and 15.9 ppm.

Given the very low NB concentration and the near-zero absorbance of NB at the LED wavelength, the photovoltage reduction cannot be attributed to optical absorption by the NB[21]. The PL quenching in the presence of NB can be attributed to the interaction between the electron-poor benzene ring of the NB and the amino group of the EDA with the consequent formation of a Meisenheimer complex. This sensing mechanism was already demonstrated, and other luminescent devices based on amine-ligated QD showed remarkable selectivity towards NACs[18,21]. Further selectivity analysis and the evaluation of the sensor performance under different environmental conditions are still being carried out and will be discussed in a future work.

Fig. 4b shows the sensor's response upon repeated exposures to increasing NB concentrations. NB concentration was controlled by increasing the temperature of the NB reservoir, while keeping the sensor at room temperature.

The photovoltage variation was clearly correlated to the NB concentration and full baseline recovery was observed after every exposure to the NB gas. A plot of the sensor response vs. NB concentration (Fig. 5a) shows a non-linear trend. This effect can be attributed to the saturation of the amine ligands by the NB molecules, thus showing that the proposed device is best suited for operation at very low gas concentrations. Assuming a proportionality between NB concentration and the sensor response in the 1 ppb – 1 ppm range, a rough estimation of the sensor detection limit was obtained. The sensor noise was measured as the standard deviation of the photovoltage over a 5-minute measurement without NB. The detection limit was calculated as

the minimum NB concentration for which a variation of the photovoltage three times higher than the noise could be expected (signal to noise ratio of 10 dB). With this approach, a detection limit of 10 ppb was estimated. Considering the molecular weight, density, and vapor pressure of NB, we can estimate that our device should be able to detect the NB gas released by 42 nl of NB in a closed 1 l container[22]. Such high sensitivity is suitable for practical indoor applications such as safety and security assessment in critical environments. Even if further investigations are needed to experimentally confirm the estimated detection limit, the proposed device already showed outstanding performance if compared to other NAC vapor detectors based on QD.

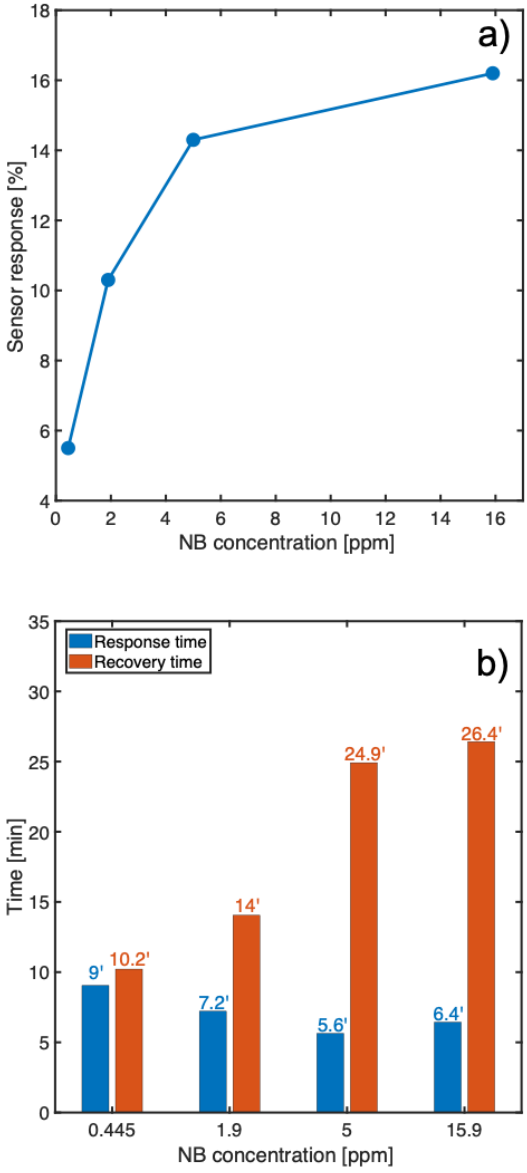

FIG. 5. (a) Sensor response vs. NB concentration. (b) Response time and recovery time vs. NB concentration.

Fig. 5b shows the measured response and recovery time for the different NB concentrations. Response showed a weak dependence on the NB concentration, with a minimum time of 5.6 minutes at 5 ppm. The recovery time monotonically increased with the NB concentration. This behavior is expected, since at higher concentration more time is needed to desorb the NB molecules from the surface of the QD.

In conclusion, we fabricated a sensor based on PL PbS QDs and commercial electronic devices (a blue LED and a NIR photodetector) for NAC detection. NB was chosen as a representative NAC and sensor response was measured at different NB concentrations. The sensor showed outstanding sensitivity with a response S=10.3% upon exposure to 1.9 ppm of NB and a response time of 7.2 minutes. Recovery time was 14 minutes. The sensor detection limit was estimated as low as 10 ppb, a value lower than any other NAC vapor sensor

based on QD reported in literature. Full sensor recovery was obtained even after several exposures to NB gas. The proposed system showed high sensitivity, low cost and has small footprint, thus it has the potentiality to become part of highly distributed sensor networks for safety and security applications.

ACKNOWLEDGMENTS

Carlo Giansante thanks Progetto di Ricerca MIUR PON 2014-2020, Energia per l'Ambiente TARANTO (Project Number: ARS01_00637).

DATA AVAILABILITY

The data that support the findings of this study are available from the corresponding author upon reasonable request.

[1] F. Akhgari, H. Fattahi, and Y.M. Oskoei, Sens. Actuators B Chem. **221**, 867 (2015).
[2] J.S. Caygill, F. Davis, and S.P.J. Higson, Talanta **88**, 14 (2012).
[3] S. Singh, J. Hazard. Mater. **144**, 15 (2007).
[4] W. Zhang, Y. Tang, A. Shi, L. Bao, Y. Shen, R. Shen, and Y. Ye, Materials **11**, 1364 (2018).
[5] S.J. Toal and W.C. Trogler, J. Mater. Chem. **16**, 2871 (2006).
[6] Y. Ma, S. Wang, and L. Wang, TrAC Trends Anal. Chem. **65**, 13 (2015).
[7] X. Sun, Y. Wang, and Y. Lei, Chem. Soc. Rev. **44**, 8019 (2015).
[8] K.C. To, S. Ben-Jaber, and I.P. Parkin, ACS Nano **14**, 10804 (2020).
[9] J.Y. Kim, O. Voznyy, D. Zhitomirsky, and E.H. Sargent, Adv. Mater. **25**, 4986 (2013).
[10] C.R. Kagan, E. Lifshitz, E.H. Sargent, and D.V. Talapin, Science **353**, aac5523 (2016).
[11] V. Galstyan, Anal. Chim. Acta **1152**, 238192 (2021).
[12] R. Tu, B. Liu, Z. Wang, D. Gao, F. Wang, Q. Fang, and Z. Zhang, Anal. Chem. **80**, 3458 (2008).
[13] A. Nguyen, C.M. Gonzalez, R. Sinelnikov, W. Newman, S. Sun, R. Lockwood, J.G.C. Veinot, and A. Meldrum, Nanotechnology **27**, 105501 (2016).
[14] Z. Wu, H. Duan, Z. Li, J. Guo, F. Zhong, Y. Cao, and D. Jia, Sensors **17**, 2676 (2017).
[15] D.G. Babar and S.S. Garje, ACS Omega **5**, 2710 (2020).
[16] Y. Zheng, ·Shu Wang, R. Li, L. Pan, L. Li, Z. Qi, and C. Li, Res. Chem. Intermed. **47**, 2421 (2021).
[17] C. Giansante, J. Phys. Chem. C **122**, 18110 (2018).
[18] X. Tian, H. Peng, Y. Li, C. Yang, Z. Zhou, and Y. Wang, Sens. Actuators B Chem. **243**, 1002 (2017).
[19] F. Mitri, A. De Iacovo, S. De Santis, C. Giansante, G. Sotgiu, and L. Colace, ACS Appl. Electron. Mater. acsaelm.1c00401 (2021).
[20] E.J. Lynch and C.R. Wilke, J. Chem. Eng. Data **5**, 300 (1960).
[21] K. Zhang, H. Zhou, Q. Mei, S. Wang, G. Guan, R. Liu, J. Zhang, and Z. Zhang, J. Am. Chem. Soc. **133**, 8424 (2011).
[22] M.R. Eslami and N. Alizadeh, Sens. Actuators B Chem. **278**, 55 (2019).

a)

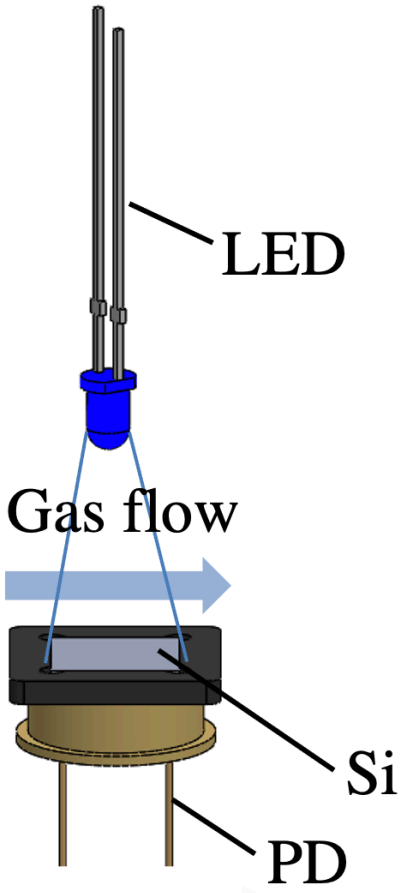

b)

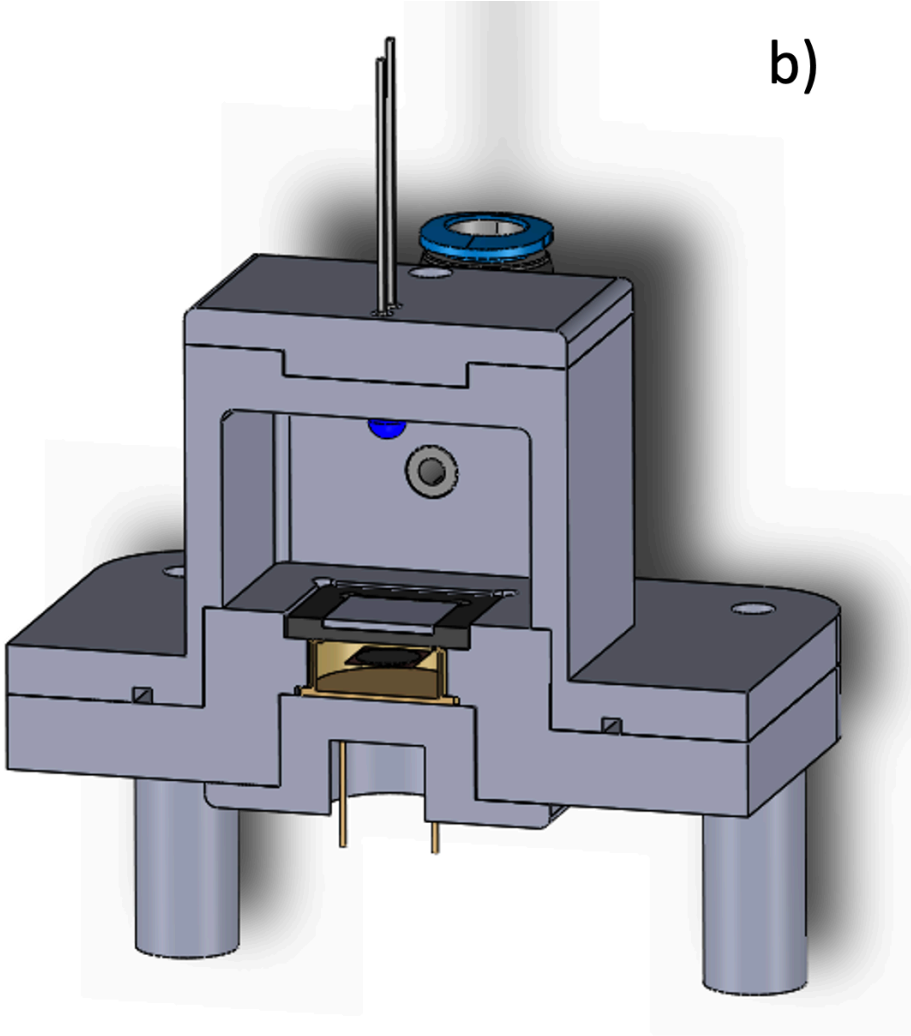

c)

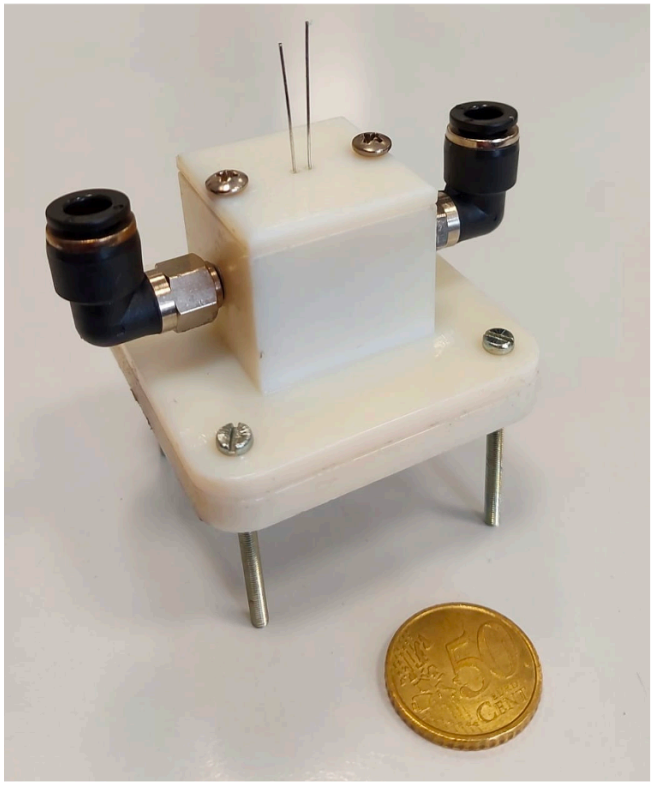

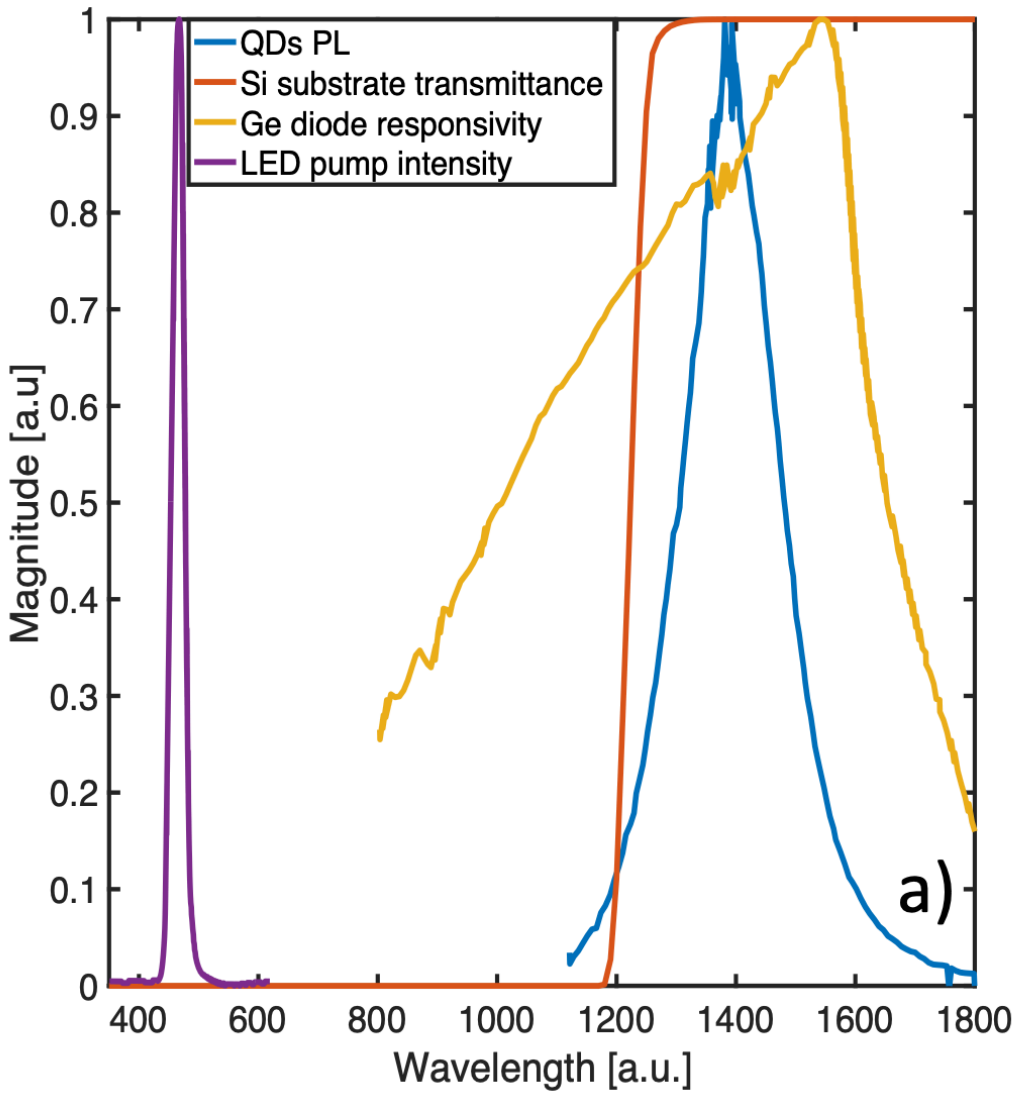
QDs PL
Si substrate transmittance
Ge diode responsivity
LED pump intensity
Magnitude [a.u]
Wavelength [a.u.]
a)

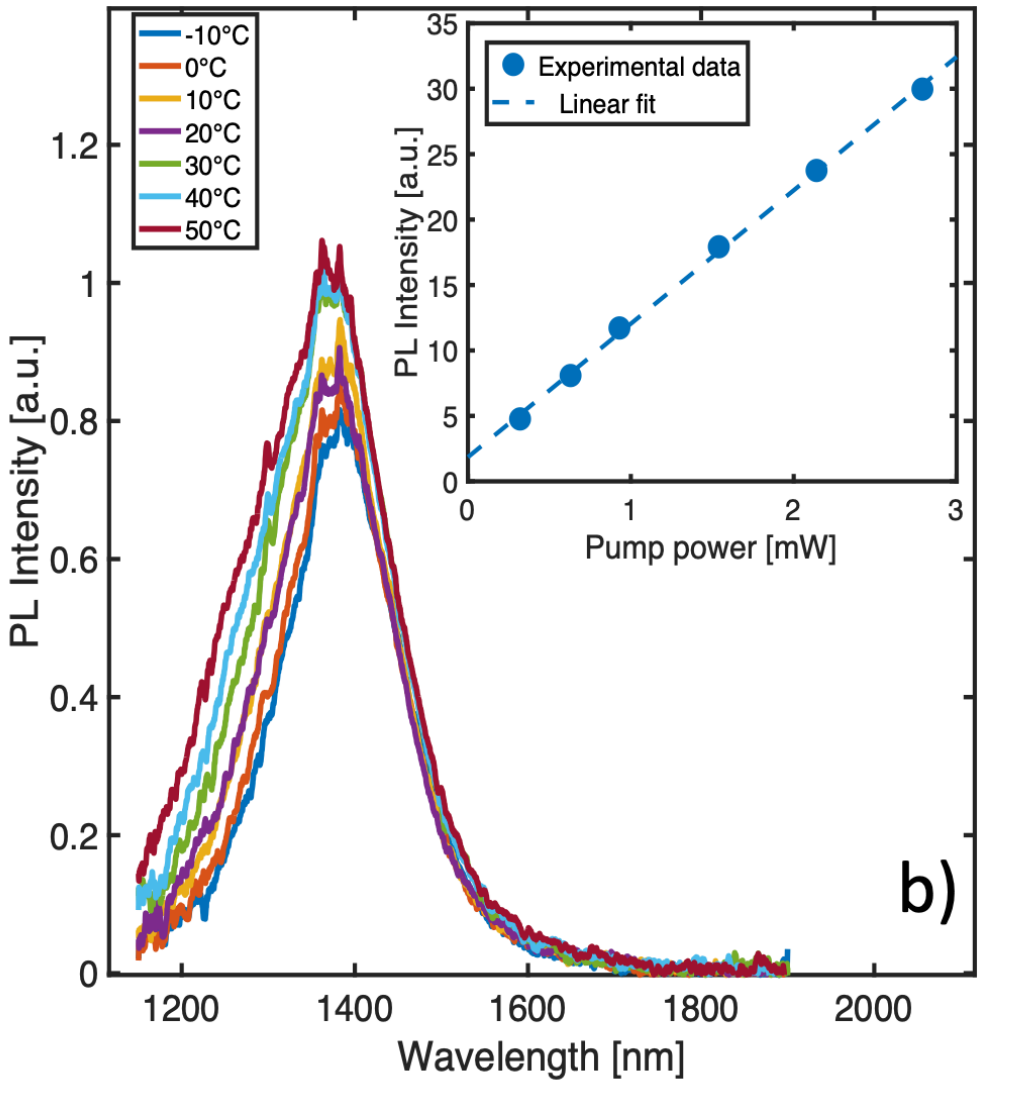
-10°C
0°C
10°C
20°C
30°C
40°C
50°C
PL Intensity [a.u.]
Wavelength [nm]
Experimental data
Linear fit
PL Intensity [a.u.]
Pump power [mW]
b)

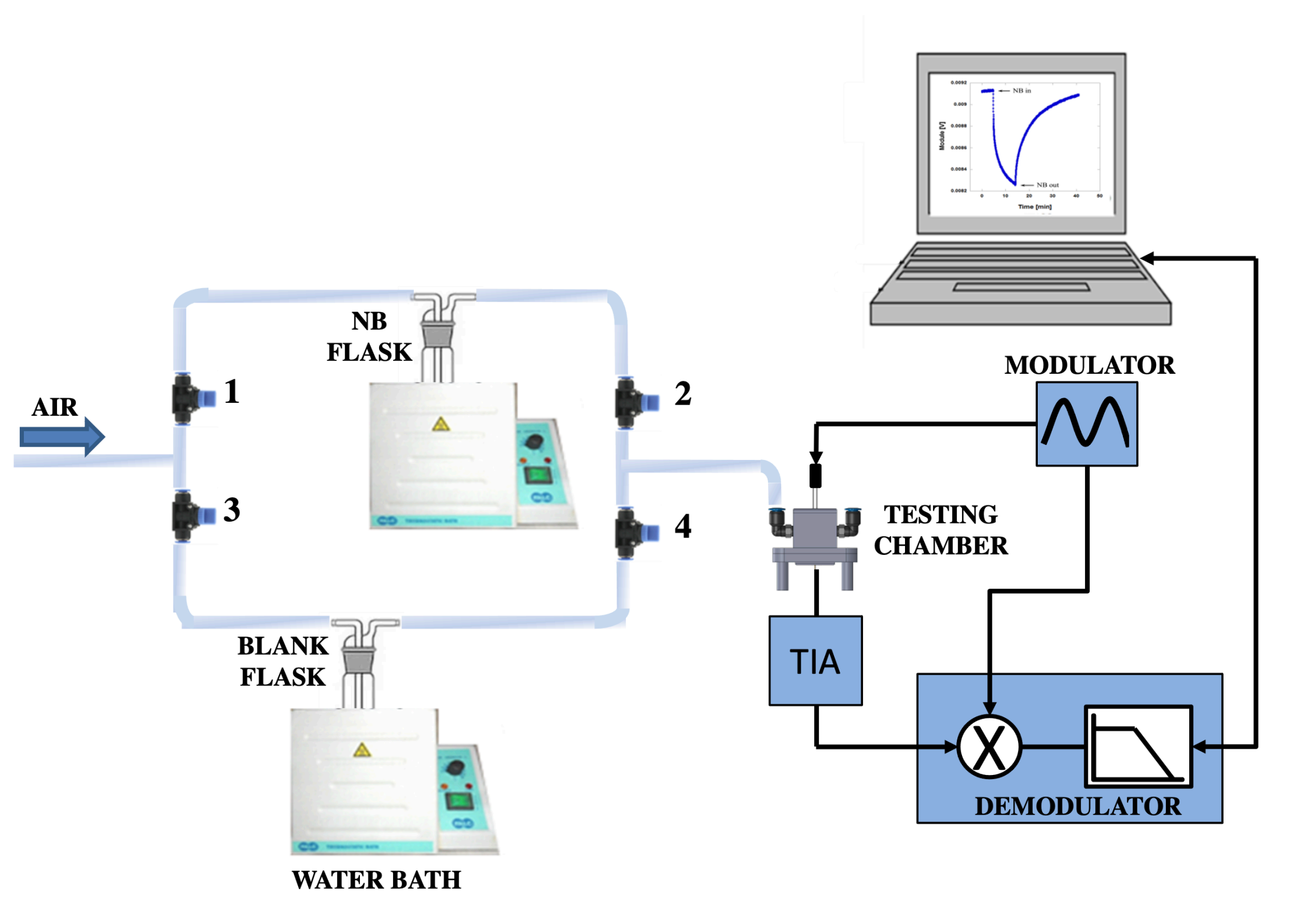
NB in
NB out
Module [V]
Time [min]
NB
FLASK
AIR
1
2
3
4
MODULATOR
TESTING
CHAMBER
TIA
BLANK
FLASK
DEMODULATOR
WATER BATH

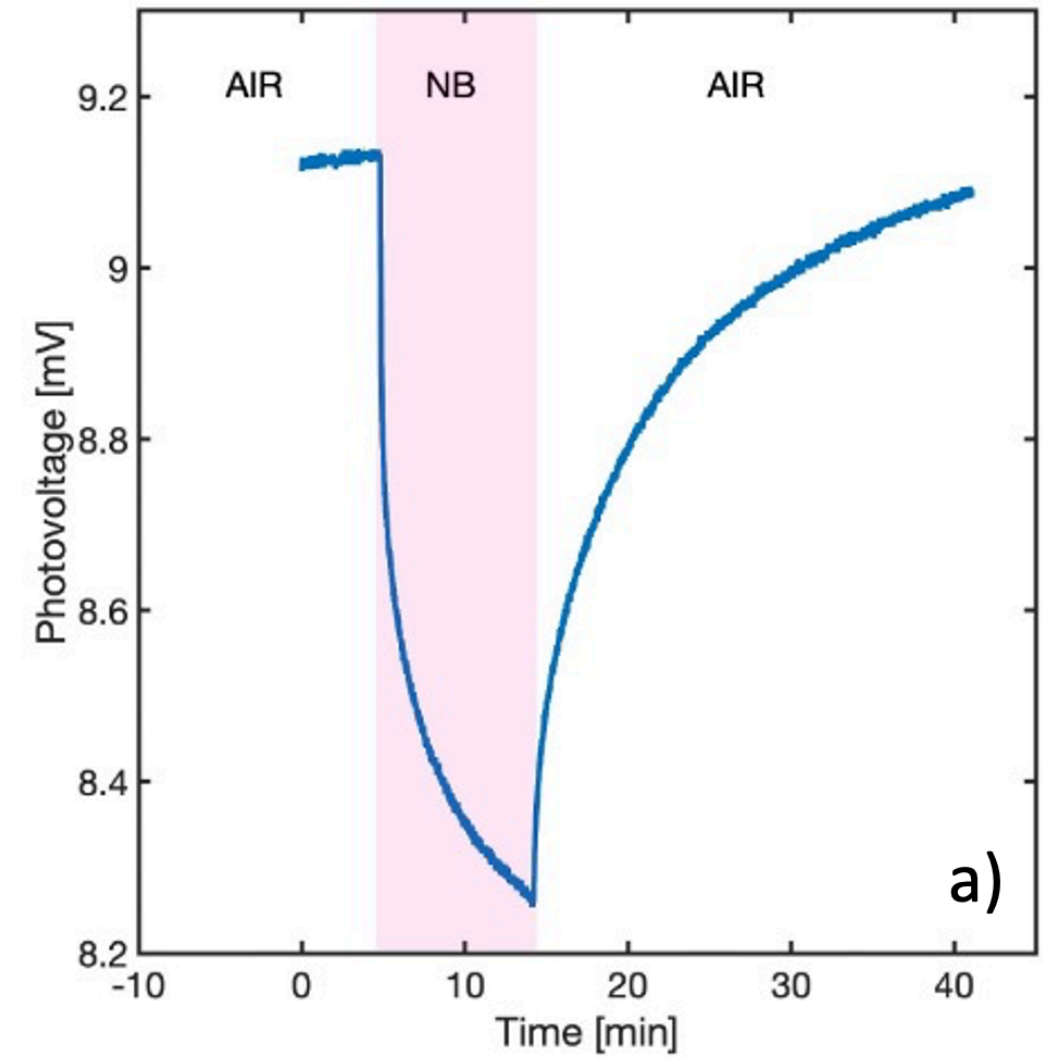
AIR
NB
AIR
9.2
9
8.8
8.6
8.4
8.2
Photovoltage [mV]
-10
0
10
20
30
40
Time [min]
a)

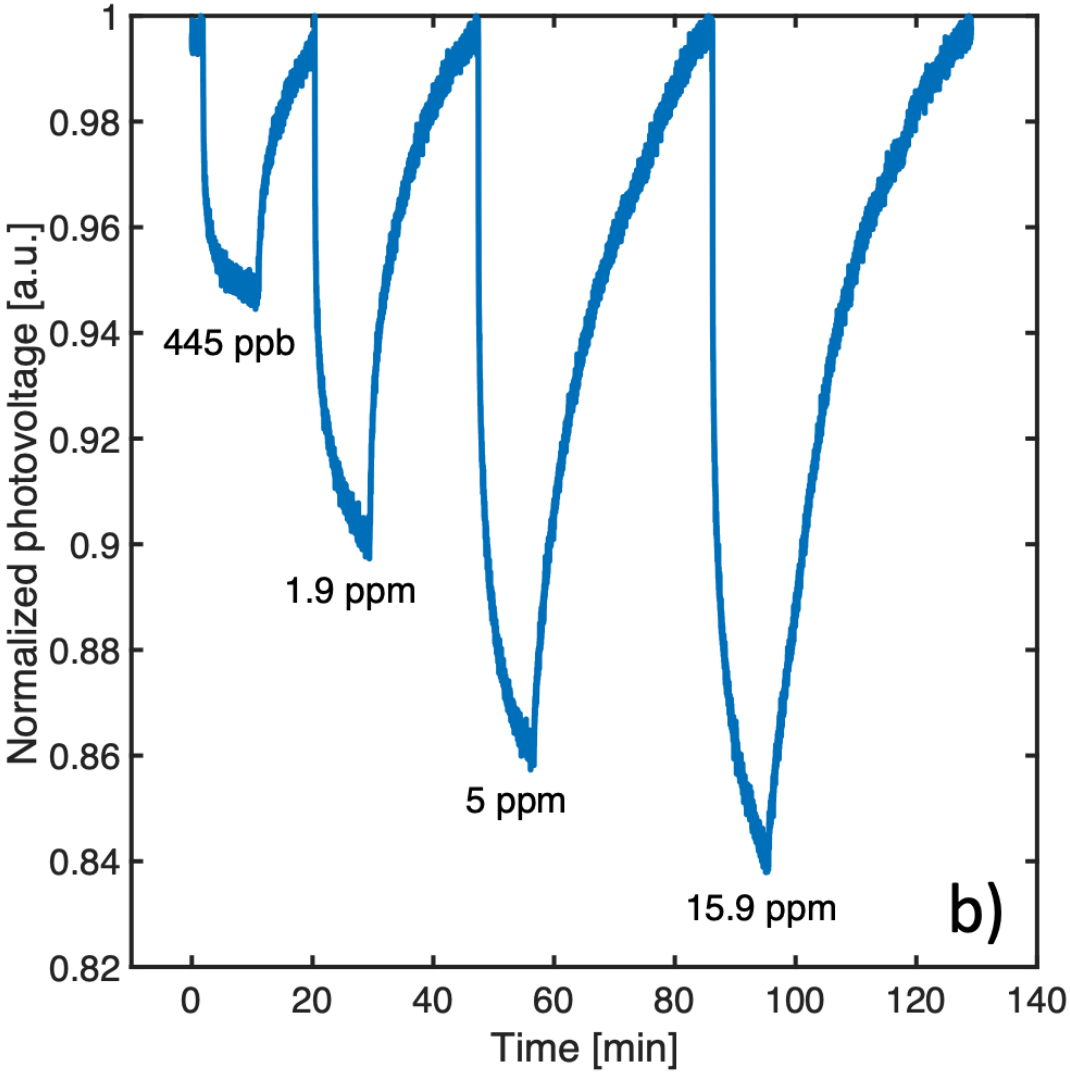
1
0.98
0.96
0.94
0.92
0.9
0.88
0.86
0.84
0.82
Normalized photovoltage [a.u.]
445 ppb
1.9 ppm
5 ppm
15.9 ppm
0
20
40
60
80
100
120
140
Time [min]
b)

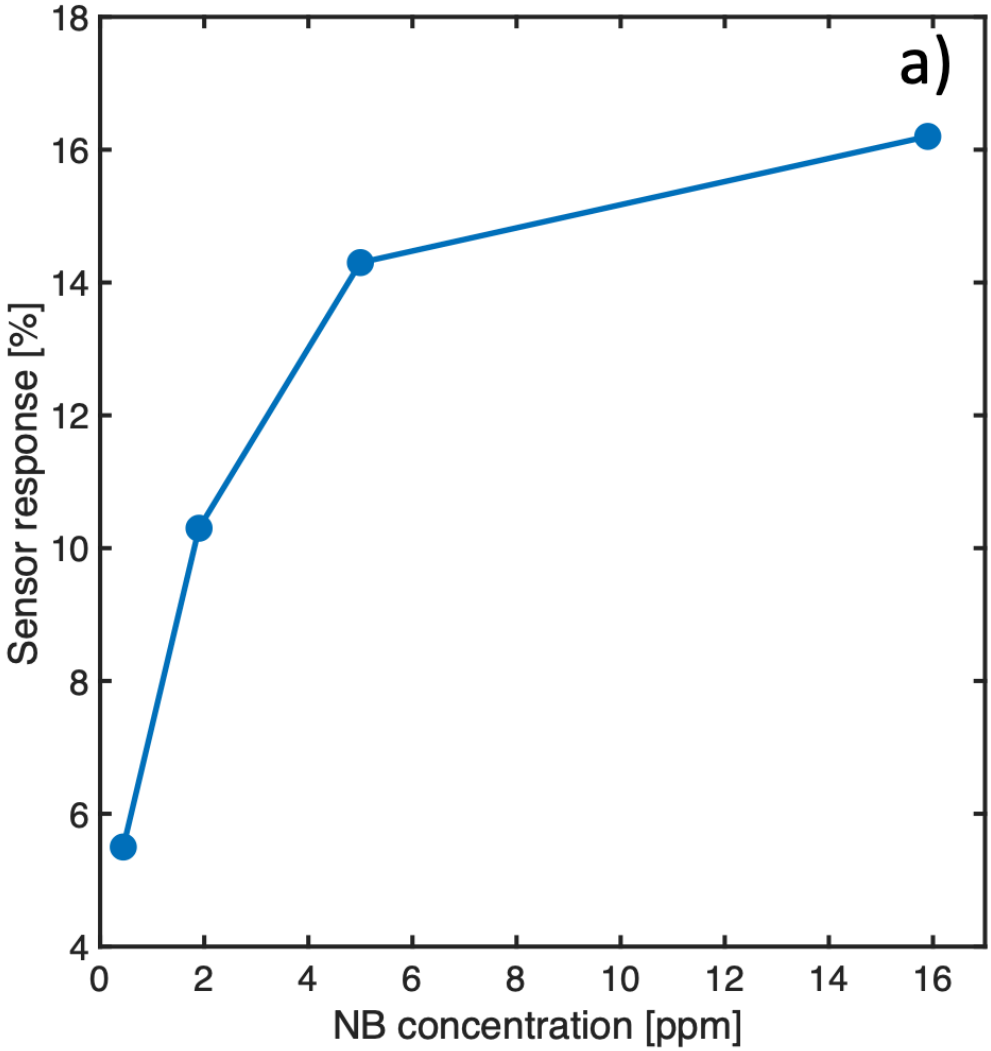
a)
Sensor response [%]
NB concentration [ppm]
18
16
14
12
10
8
6
4
0
2
4
6
8
10
12
14
16

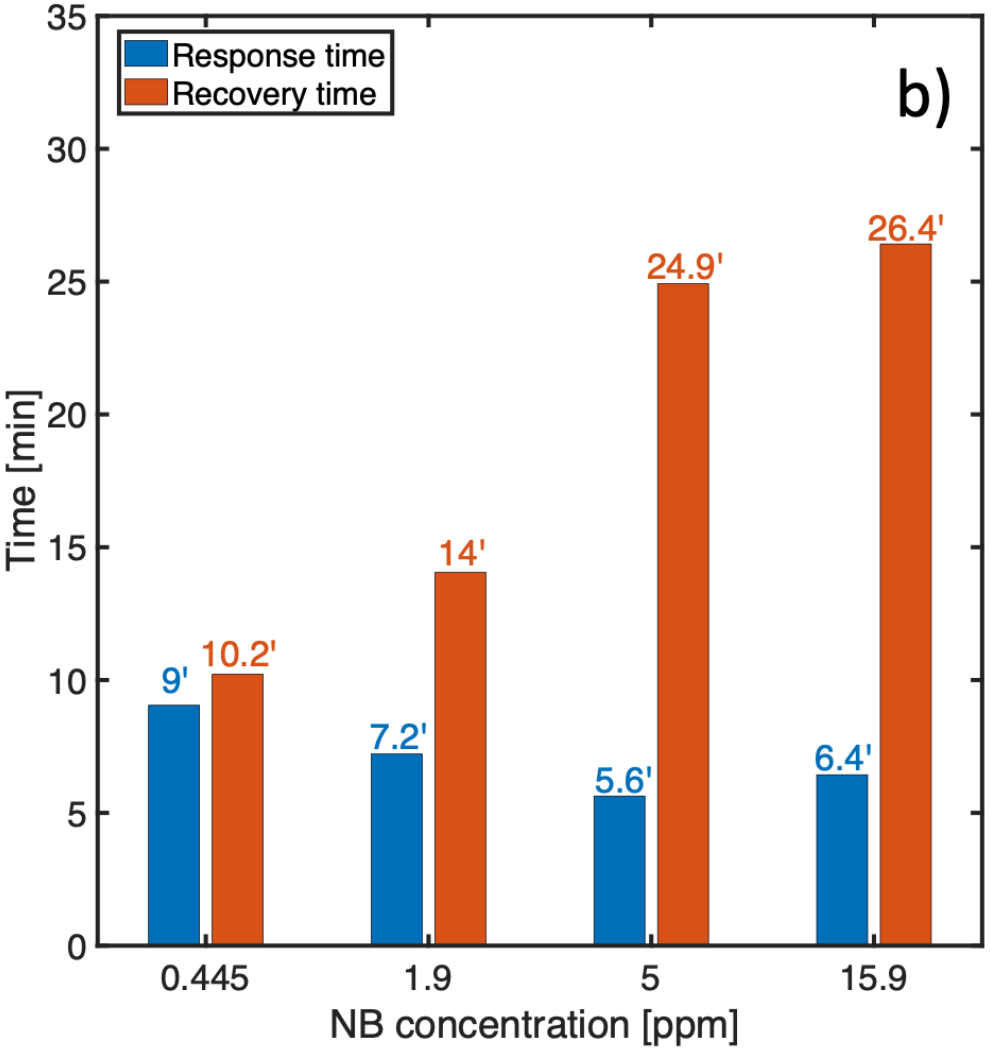
b)
Response time
Recovery time
Time [min]
NB concentration [ppm]
35
30
25
20
15
10
5
0
0.445
1.9
5
15.9
9'
10.2'
7.2'
14'
5.6'
24.9'
6.4'
26.4'